Microstructural analysis of oriented cores in Bou El Jaj district (Hercynian Central Massif, Morocco)

Análisis microestructural de testigos orientados en el distrito de Bou El Jaj (Macizo Hercínico Central, Marruecos)

El Mustapha Seghir[1,2], Hmidou El Ouardi[1] and Jeffrey Lindhorst[2,3]

[1] CartoTec, University Moulay Ismail, FSM, Department of Geology, PB.. 11201 Zitoune, Meknes, Morocco. sempha@gmail.com; h.elouardi@fs-umi.ac.ma;
[2] Kasbah Resources Limited, 11 Moreau Mews, Applecross WA 6153 Australia. mseghir@kasbahresources.com
[3] Gruvan Group International, Kigali Rwanda. jeffrey@gruvangroup.com.

ABSTRACT

This paper presents the microtectonic study based on oriented thin sections, one of the keys to understand the structural model proposed in the Bou El Jaj (BLJ) sector, located in the NE termination of the Central Hercynian massif of Morocco. Oriented thin sections from a variety of structural domains based on bedding and structures orientation have been examined from around the two prospects of the (BLJ) tin deposit in order to determine the deformation history of these rocks hosting this ore body. Three ductile deformation phases have been detected and one brittle deformation characterized by extensional jogs associated with conjugate tourmalinzed structures oriented N035 and N070.

Key-words: *Microtectonic analysis, tin mineralization, Bou El Jaj district, Central Hercynian massif, Morocco.*

RESUMEN

Este artículo presenta el estudio microtectónico basado en láminas delgadas orientadas, uno de los elementos claves para entender el modelo estructural propuesto para el sector de Bou El Jaj (BLJ), situado en la terminación NE del macizo Hercínico Central de Marruecos. En las láminas delgadas orientadas procedentes de dos prospecciones de los yacimientos de estaño se ha determinado la estratificación y las orientaciones de las estructuras con vistas a determinar la historia deformacional de la roca encajante. Se han determinado tres fases de deformación dúctil y una frágil caracterizada por venas extensionales asociadas a estructuras conjugadas orientadas N035 y N070 y rellenas de turmalina.

Palabras clave: *Análisis microtectónico, mineralización de estaño, distrito de Bou El Jaj, macizo Hercínico Central, Marruecos.*

Geogaceta, 63 (2018), 115-118
ISSN (versión impresa): 0213-683X
ISSN (Internet): 2173-6545

Recepción: 30 de enero de 2017
Revisión: 9 de abril 2017
Aceptación: 26 de abril 2017

Introduction

The Bou El Jaj (BLJ) area is located in the north-eastern part of the Moroccan Central Hercynian massif (CHM). (Fig. 1a). The geological studies that have been focused on this region correspond mainly to magmatism and mining geology. Studies on structural geology and geological mapping began to develop in order to support mining prospecting for tin and fluorite. This work deals with a microtectonic analysis based on the study of thin sections of samples in several cores, allowing us to refine the interpretative structural model of the region. Microscopic examination of oriented thin section is useful for defining overprinting relationships because it reveals features not visible or that are unclear at larger scales. An additional aim was to characterize a range of structural domains to define how they formed. Examining samples from a wide range of structural domains maximizes the number of structural relationships that can be observed giving a more comprehensive understanding of the structural history. We present the results of seven oriented thin section of drilling cores from two prospects (Ain Karma "AK" and Hill 982). The observed microstructures permit to understand the deformation history in the sector and the relationships between deformations and tin mineralization.

Geological setting

The area study of Bou El Jaj is located in the western edge of the Fourhal basin, near the NE-SW Smaala Oulmes fault zone bordering the anticlinal ridge of El Hammam (Fig. 1b). The Fourhal basin is characterized by thick sedimentary series of the Upper Visean-Namurian, composed of flysch organized in turbidite sequences. These sediments are constituted by phyllitic shales and fine sandstones (psammite) with occasional interbedded limestone layers (Michard, 1976; Tahiri, 1994; Rahho, 1996; Izart *et al.*, 2001). The sedimentary rocks are intruded by igneous sills, composed of rhyolites, gabbros and diabase. The BLJ district is characterized by the presence of tourmalinite veins mainly oriented NE-SW with a dip generally towards the NW. This tourmaline mineralization stretches over 8 km from Bou El Jaj in the south to the large Achmmach tin deposit in the north (Barodi y Chbihi, 1998; Fettouhi and Qalbi, 2002, Fig. 1c). The geological and mining works of both the western sector (El Hammam) and the eas-

Copyright© 2018 Sociedad Geológica de España / www.geogaceta.com

tern sector (Achmmach and BLJ) all agree that fluorite and tin mineralizations occurred in the context of dextral shears, having generated *en echelon* jogs oriented NE-SW.

The detailed geological survey of the BLJ sector based on geological and mining mapping, drilling holes data and micro-tectonic analysis on thin oriented sections allowed us to show the relationship between deformations and ore deposits and to specify their mode of deposit.

Structures

In the BLJ district, geological structures oriented NE-SW, resulting from several episodes of deformation, are characteristic of a fold-and-thrusts, comprising open folds with SE vergence to tight chevron folds (Fig. 1b). Brittle deformation consisting of fault planes are extensive, dipping shallowly to the NW and are interpreted as the result of SE verging thrusts. The host formation consists of interbedded turbiditic siltstone and sandstone beds steeply dipping to the WNW (~60°/295°). The strata are cross cut by felsic and mafic intrusive sills and dikes (Fig. 1b). The dikes do not show evidence of overprinting deformation. Three ductile deformation and one brittle deformation phases predating mineralization have been detected. Breccias, associated with brittle deformation and mineralization, are several meters wide and show complete primary textural destruction, with a strong sigmoidal or anastomosing shear fabric.

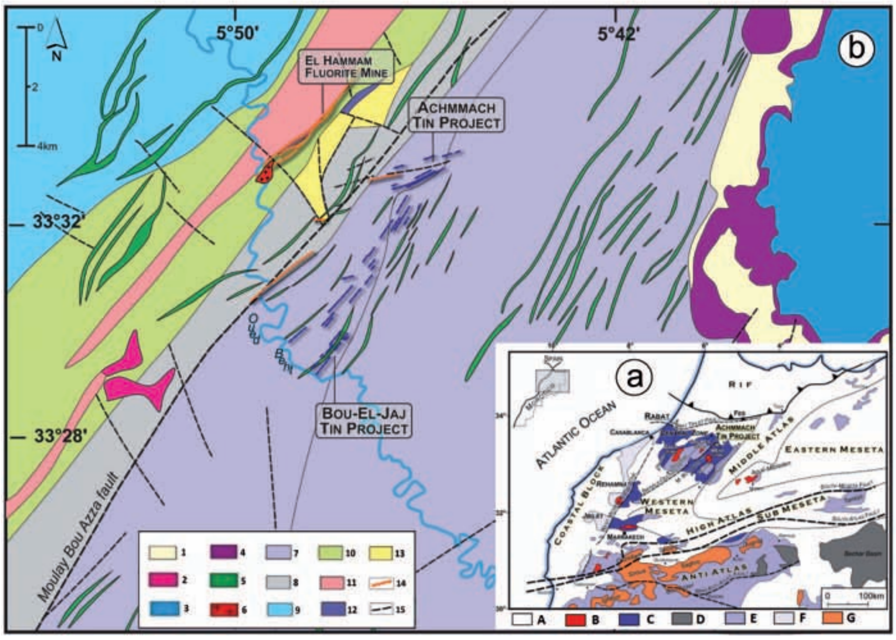

Fig. 1.- Regional geology from the regional to the prospect scale. a) Variscan outcrops in Morocco: A- post Paleozoic rocks; B- Hercynian granite; C- Western Meseta carboniferous basins; D- Anti Atlas carboniferous basins; E- Anti Atlas and Western Meseta, Cambrian Devonian; F- Western Meseta and coastal block, Cambrian; G- Precambrian rocks. b). Local geology of the study area: 1- Cover; 2- Tephrite- Plio-quaternary volcanism; 3- Liassic Dolomites; 4- Triassic Basalt; 5- Permian dolerite; 6- Monzogranite of Oued Beht; 7- Upper Visean Interbedded sandstone and shale; 8- Upper to Middle Visean Posidonomya turbidite; 9- Lower Visean schist , interbedded sandstones and limestones; 10- Lower Visean-Tournisean- schist, conglomerate and limestones rocks; 11- Devonian limestones; 12- Silurian graptolitic black schist; 13- Ordovician quartzite and schist; 14- Fluorite veins; 15- Tourmaline lodes. Modified from Piqué and Michard (1989) and Hoepffner *et al.* (2005). See color figure in the web.

Fig. 1.- Geología del sector estudiado a escalas regional y local. a). Afloramientos variscos en Marruecos: A- rocas post-paleozoicas; B- granito hercínico; C- cuencas carboníferas de la Meseta Occidental; D- cuencas carboníferas del Anti Atlas; E- Cámbrico-Devónico del Anti Atlas y de la Meseta Occidental; F- Meseta Occidental y bloque costero del Cámbrico; G- rocas precámbricas. b). Geología local de la zona de estudio; 1- cobertera; 2- tefrita, volcanismo Plio-Cuaternario; 3- dolomía del Lías; 4- basalto triásico; 5- dolerita pérmica; 6- monzogranito de Oued Beht; 7- areniscas y lutitas del Viseense superior; 8- turbidita de Posidonomyas del Viseense medio-superior; 9- areniscas y calizas del Viseense superior; 10- esquistos, conglomerados y calizas del Viseense inferior-Tournaisiense; 11- calizas devónicas; 12- esquistos negros graptolíticos del Silúrico; 13- cuarcitas y esquistos ordovícicos; 14- venas de fluorita; 15- menas de turmalina. Modificado de Piqué y Michard (1989) y Hoepffner et al. *(2005). Ver figura en color en la web.*

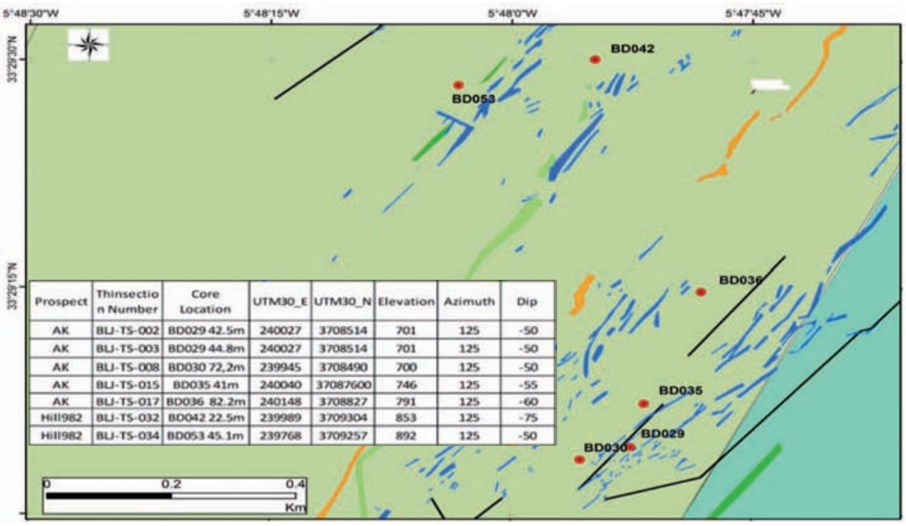

Prospect	Thinsection Number	Core Location	UTM30_E	UTM30_N	Elevation	Azimuth	Dip
AK	BLJ-TS-002	BD029 42.5m	240027	3708514	701	125	-50
AK	BLJ-TS-003	BD029 44.8m	240027	3708514	701	125	-50
AK	BLJ-TS-008	BD030 72,2m	239945	3708490	700	125	-50
AK	BLJ-TS-015	BD035 41m	240040	37087600	746	125	-55
AK	BLJ-TS-017	BD036 82.2m	240148	3708827	791	125	-60
Hill982	BLJ-TS-032	BD042 22.5m	239989	3709304	853	125	-75
Hill982	BLJ-TS-034	BD053 45.1m	239768	3709257	892	125	-50

Fig. 2.- Location of drilling core oriented samples from which thin sections were obtained and table with localization and orientation details. See color figure in the web.

Fig. 2.- Localización de los sondeos a partir de los cuales se han obtenido las muestras utilizadas para la realización de las láminas delgadas y tabla con los detalles de localización y orientación. Ver figura en color en la web.

Microstructures

A variety of samples were carefully selected from the core sampling in two localities: Ain Karma (AK) and Hill 982 (Fig. 2), in order to determine the deformation history of rocks hosting the ore body and to complement our field observations by the study of subsurface microstructures.

The study of thin sections shows that S1 is sub-parallel to S0 (Phase D1) (Figs. 3a, 4a and 6a); S2 is axial planar crenulation cleavage related to chevron folds affecting S1 (Phase D2) (Figs. 3a, 4d and 6b); D3 corresponds to the shallow ly west-dipping thrust, which produced displacement of the quartz veinlet (Figs. 3b, 4b, 4d and 6c); and the ductile deformation phases are overprinted by brittle structures associated with some quartz-sulphide-tourmaline-cassiterite-carbonate veins with infill textures (Fig. 3c).

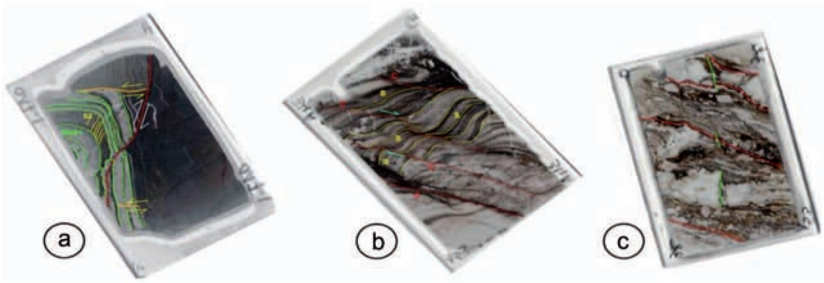

Fig. 3- Thin sections showing the structural features in BLJ. a) sample 017-1: microfold affecting S0/S1, S2 crenulation cleavage and a reverse fault that shows the fold-and-thrust structure. b) Sample 34-A: shallowly dipping C-S structure with dextral sense. c) Sample 32: brittle-ductile , shallowly dipping structure. See color figure in the web.

Fig. 3.- Láminas delgadas que muestran las estructuras representativas de la BLJ. a) muestra 017-1: micropliegue afectando a S0/S1, crenuladas por S2, y falla inversa que muestra la estructura de pliegues y cabalgamientos. b) Muestra 34-A: estructura C-S con buzamiento suave y sentido de movimiento dextro. c) Muestra 32: estructura frágil-dúctil con buzamiento suave. Ver figura en color en la web.

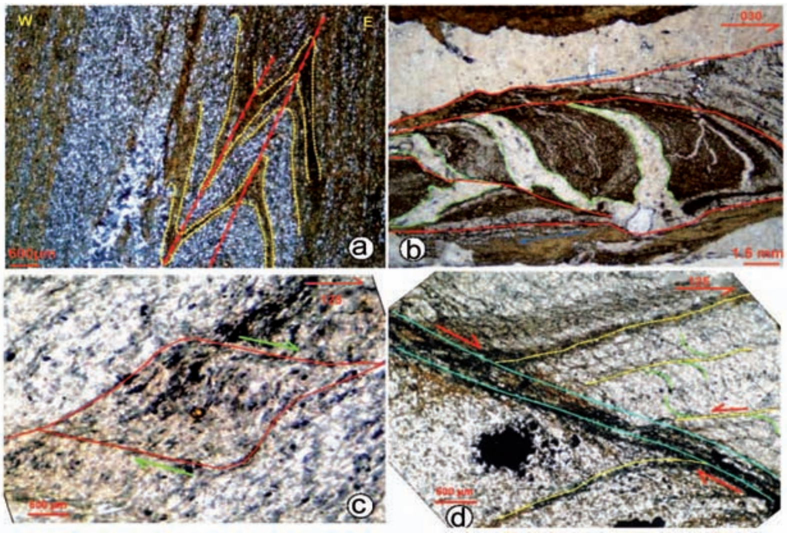

Fig. 4- Microscope photographs of some structural features. a) Sample 017-1: microfold affecting S0/S1, thickening in the fold hinge; b) sample 008-2: dextral shear zone with crown milky quartz; c)- sample 32-2: shallowly dipping shear zones cross cutting the bedding; d) sample 34A-2: tourmaline vein (marked with cyan lines) affected by a shallowly dipping dextral shear zone with tin mineralization with S0/1 with yellow colour, S2 in blue colour. See color figure in the web.

Fig. 4- Fotografías de microscopio de algunas estructuras. a) muestra 017-1: micropliegue afectando a S0 y S1, engrosamiento en la charnela; b) muestra 005-2: zona de cizalla con buzamiento bajo dextra con cuarzo lechoso; c) muestra 32-3: fábrica de cizalla somera cortando la estratificación; d) muestra 34A-2: vena de turmalina afectada por zizalla dextra que contiene mineralización de estaño ; S0/S1 y S2 están marcadas, por líneas de color amarillo y azul, respectivamente.. Ver figura en color en la web.

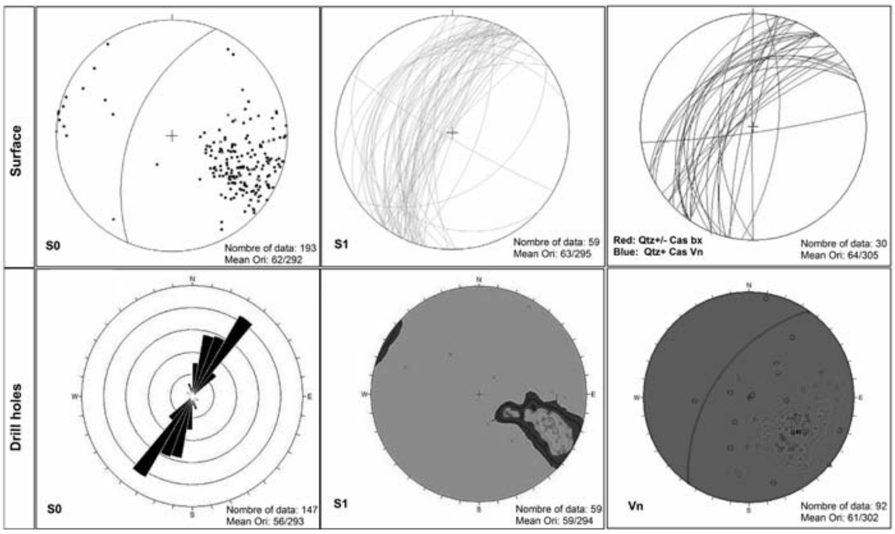

Fig. 5.- Stereoplots of structural features (S0 stratification, S1 schistosity and veins) obtained from the surface (top row) and from the drilling core (bottom row). See color figure in the web.

Fig. 5.- Proyección estereográfica de elementos estructurales (estratificación S0, esquistosidad S1 y venas) obtenidas en superficie (parte superior) y en el sondeo (parte inferior). Ver figura en color en la web.

Conjugate C-S structures formed extensional jogs that control the formation of tourmaline and west fragments of milky quartz and tourmalinite have a round shape according to the brittle-ductile deformation (Figs. 3c, 4b and 6b).

The stereographic projections of S1 are very similar to those of S0 with almost identical mean orientation and smaller poles dispersion Considering the tight nature of the chevron folds observed in the field, S1 is parallel to core axes. The veining have an orientation of 035 not exactly parallel to S0/S1, which are 020 striking.

Discussion

The structural configuration of the Palaeozoic in the whole district is the result of the Hercynian orogeny (Jebrak, 1984 ; Zerdane 1992).

The D1 phase is responsible for the district's major structuring (mega-folds with NE-SW axes). The S1 axial plane schistosity, locally developed in a weak metamorphic environment (anchizonal - epizonal), is associated with this phase.

The D2 phase, less significant than D1, develops a crenulation S2 schistosity. In the district, it is characterised by metre-sized folds on a NW-SE kink-band axis.

The D3 phase is the result of a regional ENE-WSW shortening event. The fracturing caused by this phase allowed the development of mineralized veins. Also, the NE-SW oriented P1 folds are synchronous with shear zones, whereas, P2 folds accompanied by NW-SE trending S2 cleavage are found near some faults (Tahiri 1994; Rahho 1996)

The structural model at BLJ district is inspired from the previous models and based on the field data and the microtectonic study of the drilling core.

The first ductile deformation produced east-verging folds and developed the S1 cleavage sub-parallel to S0. Resulting structures correspond to open to tight hectometric folds with SE vergence; the second ductile deformation created S2 crenulation cleavage, that corresponds to the axial plane of folds affecting S0/S1. Subsequently, S3 developed in the third ductile deformation phase, creating extensional jogs. Generally the ductile deformation generated C-S structures associated with sub-horizontal dextral shear zones. The fourth deformation phase developed under a brittle regime and created a breccia infill of silica tourmaline mineralization, which is associated with kinematic indicators that suggest dextral movement.

The deformations found at the microscopic scale reflect the same image as the field structures. The tin mineralizations are overprinting the fractured system developed during the third and fourth stages of deformations. They occur in extensional jog structures.

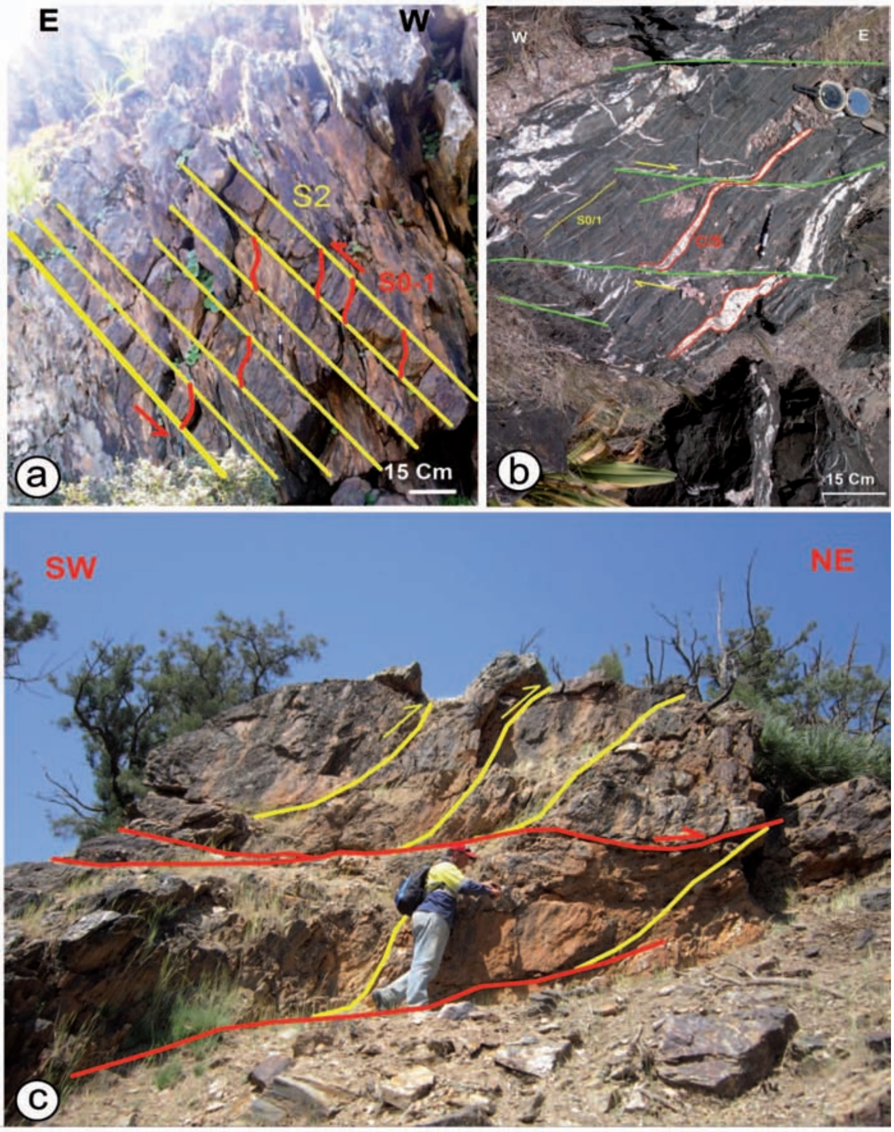

Fig. 6.- Surface structural features at the BLJ prospect area. a) relationship between S0/1 and S2; b) dextral C-S structure, E-W striking, shows extensional jogs filled of milky quartz; c) main thrust planes (red) and drag folds/secondary planes (yellow); thrusting seems to post-date sediment tourmalinitization. See color figure in the web.

Fig. 6.- Aspectos estructurales de superficie en la zona de prospección BLJ, a) relación entre S0/1 y S2; b) estructura C-S dextra con orientación E-W que muestra rellenos de cuarzo lechoso de las grietas extensionales; c) plano principal de calabalgamiento y pliegues de propagación y planos secundarios del sistema de cabalgamiento que post-datan el proceso de turmalización. Ver figura en color en la web.

Conclusions

The BLJ district shows superimposed tectonic deformations controlling the tourmaline alterations and associated tin mineralizations. According to field geological data, geological mapping and microtectonic analysis from oriented thin sections, three ductile deformation stages and one single brittle deformation stage have been detected. Ductile deformations corresponding to sub-horizontal shears are accompanied by C-S structures and pull apart structures that contain folded milky quartz. Brittle deformations corresponding mainly to sub-vertical hydrothermal breccia infill with tourmalinite fragments collapsed in the matrix and containing tin mineralization. All the three ductile deformation stages are overprinted by the tin mineralization explored at present in the sector. The same meso-structures have been found at the outcrop scale and detected under microscope analysis of the oriented thin section. The tin mineralized structures are shallowly dipping and infill tourmaline quartz cassiterite and have an extensional jog shape of these conjugate N35 and N70 structures.

Acknowledgement

This work is supported by the UMI-El Ouardi project. Authors would like to thank Kasbah Resources Limited for their support. Also many thanks to reviewers Antonio Casas and the second anonymous reviewer.

References

Barodi, E.B. and Chbihi A. (1998). *Chronique de la recherche minière.* 531–532, 55–63.

Fettouhi, A. and Qalbi, A. (2002). Achmmach Tin *Deposit, Geology, Results of Work and Evaluation of resources,* BRPM Report, 45 p.

Hoepffner, C., Soulaimani, A. and Piqué, A. (2005). *Journal of African Earh Sciences* 43, 144-165.

Izart A., Chevremont, P., Tahiri, A., El Boursoumi, A. and Thieblemont, D. (2001). *Notes et Mémoires du Service Géologique du Maroc 411 bis, Rabat.*

Jebrak, M., (1984). *Contribution à l'histoire naturelle des filons F-Ba du domaine varisque. Essai de caractérisation structurale et géochimique des filons en extension et en décrochements. Massifs centraux français et marocains.* Thèse d'Etat. Univ. Orléans, 470 p.

Michard, A. (1976). *Notes et Mémoires du Service Géologique du Maroc 252, Rabat.*

Piqué, A. and Michard, A. (1989). *American Journal of Science* 289, 286-330.

Rahho, H. (1996). *Etude géologique du paléozoïque d' El Hammam. Analyse de lafracturation et relation avec les structures minéralisées (Maroc Central Septentrional).* Thesis, Univ. Mohamed V Rabat, *219 p.*

Tahiri, A. (1994). *Bulletin de l'Institut Scientifique de Rabat* 18, 125–144.

Zerdane, A., (1992). *Etude structurale et métallogénique des deux índices stannifères de Boueljaj et d'Achemeche.* Rapport interne de BRPM, 64p.